Self-Aligned Growth of Hexagonal TiO_2 Nanosphere Arrays on α-MoO_3 (010) Surface

Hua Gui Yang and Hua Chun Zeng*

Department of Chemical and Environmental Engineering, Faculty of Engineering, National University of Singapore, 10 Kent Ridge Crescent, Singapore 119260

Received May 2, 2003. Revised Manuscript Received June 18, 2003

At present there are two basic types of self-assembly of inorganic nanomaterials: surfactant-assisted organization and patterned-substrate deposition. In this paper, we report a novel assembled scheme for fabrication of hexagonal superlattice arrays of anatase TiO_2 nanospheres on the (010) crystal plane of α-MoO_3 without the assistance of organic surfactants or substrate prefabrication. The growth and self-assembly of TiO_2 nanospheres take place simultaneously under hydrothermal conditions at 150−200 °C according to a continuous self-aligned process in which the localized enrichment of hydrolysis product HF (TiF_4 is the precursor for TiO_2) is believed to play a crucial role in initiating the self-alignment. This "growth-cum-assembly" mechanism has also been validated with our various growth experiments and materials characterization. Key synthetic parameters have been identified and future explorations have been suggested for this ordered scheme.

Introduction

Over the past decade, assembly and alignment of nanostructured oxide and other inorganic materials have attracted great research attention.[1−22] A number of solution-phase and vapor-phase methods have been developed in association with the general "bottom-up" endeavor for nanoscience and nanotechnology.[1−22] Among them, organic-surfactant-assisted assembly is the most common way to arrange nanostructured materials into ordered structures such as two-dimensional arrays or three-dimensional stack architectures.[1−9] These types of organizations normally involve preparation of colloidal solutions comprising surfactants and nanostructures in aqueous or organic solvents. A controlled drying process, including the control of drying ambience, then follows to evaporate the solvents, which decreases the interparticle/crystallite distance and forms compact nanostructured assemblies. If desired, these low-temperature nanostructures can be further heat-treated at elevated temperatures to burn out the remaining organic surfactants and solidify the prearranged structures in more permanent ways for device applications.[7]

Various geometrical arrangements have been achieved with the surfactant-assisted method. For example, linearly, squarely, and hexagonally arranged nanomaterials, including multiple layer stacking, can now be made routinely with the assistance of a variety of surfactants.[1−9] With the Langmuir−Blodgett film technique, spiral and concentric patterns of inorganic nanostructured materials have also been observed in addition to regular textural patterns.[8] Similar to the assembly of organic photonic crystals,[23−25] the organization of inorganic nanostructures with the assistance of surfac-

* To whom correspondence should be addressed. E-mail: chezhc@nus.edu.sg.

(1) Chemseddine, A.; Moritz, T. *Eur. J. Inorg. Chem*. **1999**, 235.
(2) Schärtl, W. *Adv. Mater.* **2000**, *12*, 1899.
(3) (a) Caruso, F. *Adv. Mater.* **2001**, *13*, 11. (b) Pileni, M. P. *J. Phys. Chem. B* **2001**, *105*, 3358.
(4) (a) Lin, X. M.; Jaeger, H. M.; Sorensen, C. M.; Klabunde, K. L. *J. Phys. Chem. B* **2001**, *105*, 3353. (b) Shimoda, H.; Oh, S. J.; Geng, H. Z.; Walker, R. J.; Zhang, X. B.; McNeil, L. E.; Zhou, O. *Adv. Mater.* **2002**, *14*, 899.
(5) Hassenkam, T.; Nørgaard, K.; Iversen, L.; Kiely, C. J.; Brust, M.; Bjørnholm, T. *Adv. Mater.* **2002**, *14*, 1126.
(6) Fullam, S.; Rensmo, H.; Rao, S. N.; Fitzmaurice, D. *Chem. Mater.* **2002**, *14*, 3643.
(7) Zeng, H.; Li, J.; Liu, J. P.; Wang, Z. L.; Sun, S. *Nature* **2002**, *420*, 395.
(8) (a) Kim, F.; Kwan, S.; Akana, J.; Yang, P. *J. Am. Chem. Soc.* **2001**, *123*, 4360. (b) Yang, P.; Kim, F. *Chem. Phys. Chem.* **2002**, *3*, 503.
(9) Wei, X. M.; Zeng, H. C. *J. Phys. Chem. B* **2003**, *107*, 2619.
(10) Aggarwal, S.; Monga, A. P.; Perusse, S. R.; Ramesh, R.; Ballarotto, V.; Williams, E. D.; Chalamala, B. R.; Wei, Y.; Reuss, R. H. *Science* **2000**, *287*, 2235.
(11) Gudiksen, M. S.; Lauhon, L. J.; Wang, J.; Smith, D. C.; Lieber, C. M. *Nature* **2002**, *415*, 617.
(12) Wu, Y.; Fan, R.; Yang, P. *Nano Lett.* **2002**, *2*, 83.
(13) Adelung, R.; Ernst, F.; Scott, A.; Tabib-Azar, M.; Kipp, L.; Skibowski, M.; Hollensteiner, S.; Spiecker, E.; Jäger, W.; Gunst, S.; Klein, A.; Jägermann, W.; Zaporojtchenko, V.; Faupel, F. *Adv. Mater.* **2002**, *14*, 1056.
(14) (a) Kovtyukhova, N. I.; Mallouk, T. E. *Chem. Eur. J.* **2002**, *8*, 4355. (b) Smith, P. A.; Nordquist, C. D.; Jackson, T. N.; Mayer, T. S.; Martin, B. R.; Mbindyo, J.; Mallouk, T. E. *Appl. Phys. Lett.* **2000**, *77*, 1399.
(15) Huang, S.; Dai, L.; Mau, A. W. H. *Adv. Mater.* **2002**, *14*, 1140.
(16) Masuda, Y.; Sugiyama, T.; Koumoto, K. *J. Mater. Chem.* **2002**, *12*, 2643.
(17) Thalladi, V. R.; Whitesides, G. M. *J. Am. Chem. Soc.* **2002**, *124*, 3520.
(18) Hoeppener, S.; Maoz, R.; Cohen, S. R.; Chi, L.; Fuchs, H.; Sagiv, J. *Adv. Mater.* **2002**, *14*, 1036.
(19) Michel, R.; Lussi, J. W.; Csucs, G.; Reviakine, I.; Danuser, G.; Ketterer, B.; Hubbell, J. A.; Textor, M.; Spencer, N. D. *Langmuir* **2002**, *18*, 3281.
(20) Huang, L.; Wang, Z.; Sun, J.; Miao, L.; Li, Q.; Yan, Y.; Zhao, D. *J. Am. Chem. Soc.* **2000**, *122*, 3530.
(21) (a) Martin, C. R. *Science* **1994**, *266*, 1961. (b) Lakshmi, B. B.; Dorhout, P. K.; Martin, C. R. *Chem. Mater.* **1997**, *9*, 857. (c) Lakshmi, B. B.; Patrissi, C. J.; Martin, C. R. *Chem. Mater.* **1997**, *9*, 2544.
(22) Nicewarner-Pena, S. R.; Freeman, R. G.; Reiss, B. D.; He, L.; Pena, D. J.; Walton, I. D.; Cromer, R.; Keating, C. D.; Natan, M. J. *Science* **2001**, *294*, 137.
(23) Yi, G. R.; Moon, J. H.; Manoharan, V. N.; Pine, D. J.; Yang, S. M. *J. Am. Chem. Soc.* **2002**, *124*, 13354.

10.1021/cm034313f CCC: $25.00
Published on Web 07/02/2003

tants also belongs to the "growth-then-assembly" process, where the two discrete steps, growth and assembly, can be clearly divided. To meet the future challenges imposed by rapid development of nanoscience and nanotechnology, it would also be desirable to develop "growth-cum-assembly" processes, in which the growth and assembly take place at the same time, preferably under "one-pot" or continuous synthetic conditions. In recent years, indeed, research efforts have been devoted substantially to fabrications of nanostructured material arrays on pre-patterned templates or substrates using photolithography or other chemical approaches such as electrochemical preparation of one-dimensional channels of anodic alumina membranes.[14−21] In contrast to these artificially ordered schemes, spontaneous ordering of oxide nanostructures has been attempted in recent years.[22] For example, two-dimensional PdO_2 nanoparticle arrays have been prepared from an oxidative conversion of its pure metal using the gas−solid reactions at 900 °C.[22] Nonetheless, without the substrate prefabrication, arrays of nanostructured materials with distinct geometrical arrangement and structural repetition (i.e., superlattices) have not been achieved directly on simple pristine crystal substrates so far.

In the present article we will report a novel "growth-cum-assembly" integrated process. In particular, without the assistance of organic surfactants or prefabrication of solid substrates, generation of anatase TiO_2 nanospheres and their self-alignment to hexagonal arrays on the (010) surface of orthorhombic MoO_3 (α-MoO_3) have been achieved with a "one-pot" approach under hydrothermal conditions at 150−200 °C. Apart from basic structural and chemical considerations, the selection of TiO_2−MoO_3 material system in this study is also based on its combined effects on many important applications such as photochromism and photocatalysis.[26]

Experimental Section

Dilute hydrochloric acid solution at pH = 2.1 was prepared from 1.5 M HCl solution and deionized water. Titanium tetrafluoride (TiF_4, Aldrich Chemical) was then dissolved in this solution to give a TiF_4 concentration of 0.040 M, during which the pH was changed to 1.8. The solution was clear and stable at room temperature. Deionized water was used later to adjust the TiF_4 concentration to 0.001−0.0133 M before hydrolysis reaction at elevated temperatures.

The α-MoO_3 substrate was prepared according to a previously developed flux-growth method. Briefly, single crystals of α-MoO_3 with smooth morphology were prepared from a high-temperature metal oxide flux (the molar ratio of MoO_3/Na_2MoO_4 = 85:15) at a cooling rate of 2 °C/h.[26] The platelet-like α-MoO_3 single crystals were separated from the solid-solvent Na_2MoO_4 by using a nitric acid solution (1.0 M). For the present self-assembled growth of TiO_2 nanospheres on α-MoO_3 substrate, typically, 3 pieces of high-quality α-MoO_3 crystals (average crystal size: 15 mm (length) × 2 mm (width) × 0.5 mm (thickness);[26] total weight 0.21 g, density of α-MoO_3 = 4.692 g/cm^3; estimated total surface area 2.3×10^{-4} m^2) were put into 30.0 mL of the above-prepared TiF_4 solution (in the range of 0.001−0.005 M), which was then heated in a Teflon-lined stainless autoclave at 150−200 °C for a desired period of time (2−40 h). After this hydrothermal reaction, the resulted TiO_2/α-MoO_3 samples were gently washed with deionized water and then dried naturally at room temperature. As a comparison, micro-sized α-MoO_3 crystal powder (Aldrich Chemical) was also used as substrate for the TiO_2 deposition. In this type of growth, 30.0 mL of aqueous TiF_4 solution (0.0040−0.0133 M), together with 0.30 g of α-MoO_3 microcrystals (well-faceted, i.e., single-crystalline; average crystal size: 20.0 μm × 9.1 μm × 2.2 μm, measured with SEM images; estimated total surface area 7.8×10^{-2} m^2 (This area estimation is on the lower side, because large microcrystals were used in the size measurement. Some microcrystals could be much smaller; see Supporting Information 3.)), was heated in the Teflon-lined stainless autoclave under 170 °C for 10−23 h, after which the product suspension was separated by centrifugation, followed by washing with deionized water and drying at 60 °C in an electric oven.

Crystallographic phase of TiO_2 nanospheres grown on α-MoO_3 was determined by X-ray diffraction (XRD, Shimadzu XRD-6000, Cu Kα radiation).[27] The specimen for XRD measurement was prepared by dissolving α-MoO_3 crystal powder substrate in 0.10 M NaOH solution.[26] The separated TiO_2 crystallites (undissolved in dilute NaOH) were centrifuged first and then dried at 60 °C. The surface chemical analysis of samples was made with X-ray photoelectron spectroscopy (XPS; AXIS-Hsi, Kratos Analytical) using Mg Kα X-ray source ($h\nu$ = 1253.6 eV). The XPS spectra of all studied elements, such as Ti 2p, Mo 3d, O 1s, and C 1s, were measured with a constant analyzer-pass-energy of 40 eV. All binding energies (BEs) were referenced to C 1s peak (BE = 284.7 eV) arising from adventitious carbon. The self-assembled patterns and crystal morphology of TiO_2 nanospheres were examined with scanning electron microscopy (SEM; JSM-5600LV, 15−20 kV) and transmission electron microscopy (TEM; JEM-2010, 200 kV).[27] Electron diffraction (ED) was also carried out to investigate the crystallographic orientation of TiO_2 nanospheres on the (010) surface of α-MoO_3. The TiO_2 suspension specimen for TEM imaging was prepared by dissolving α-MoO_3 substrate in 0.10 M NaOH then washed and dispersed again with deionized water in an ultrasonic water bath. Carbon-coated 200-mesh copper grids were used to support the examined samples after drying from the above TiO_2 suspension.

Results and Discussion

Site-nonselective and site-selective growths of TiO_2 nanospheres on the (010) surface of an α-MoO_3 single crystal were first investigated as a function of TiF_4 concentration (0.010−0.0010 M), temperature (50−200 °C), and reaction time (2−40 h). For syntheses with a high TiF_4 concentration ([TiF_4] ≥ 0.0020 M), the heterogeneous nucleation of TiO_2 on α-MoO_3 is nonselective. As shown in Figure 1A, a rather compact TiO_2 film on α-MoO_3 substrate was formed with a 0.0040 M TiF_4 solution after hydrothermal reaction at 200 °C for only 2 h, during which unsupported nanocrystals of TiO_2 were also readily generated in the solution phase via direct spontaneous nucleation, showing a spherical morphology (Figure 1B). With a lower TiF_4 concentration (e.g., 0.0020 M), on the other hand, similar TiO_2 thick films (not shown) and nanospheres can also be obtained at a longer reaction time (14 h, Figure 1C).

(24) Ye, Y. H.; Mayer, T. S.; Khoo, I. C.; Divliansky, I. B.; Abrams, N.; Mallouk, T. E. *J. Mater. Chem.* **2002**, *12*, 3637.

(25) Wu, H.; Thalladi, V. R.; Whitesides, S.; Whitesides, G. M. *J. Am. Chem. Soc.* **2002**, *124*, 14495.

(26) (a) Hsu, Z. Y.; Zeng, H. C. *J. Phys. Chem. B* **2000**, *104*, 11891. (b) Zeng, H. C.; Ng, W. K.; Cheong, L. H.; Xie, F.; Xu, R. *J. Phys. Chem. B* **2001**, *105*, 7178. (c) Zeng, H. C.; Xie, F.; Wong, K. C.; Mitchell, K. A. R. *Chem. Mater.* **2002**, *14*, 1788. (d) The single-crystal samples of α-MoO_3 used in the current work were examined under an optical microscope to exclude obvious crystal inhomogeneities such as visible cracks, growth steps, and habits; this was done in the same way as reported in (a) to (c).

(27) Sampanthar, J. T.; Zeng, H. C. *J. Am. Chem. Soc.* **2002**, *124*, 6668.

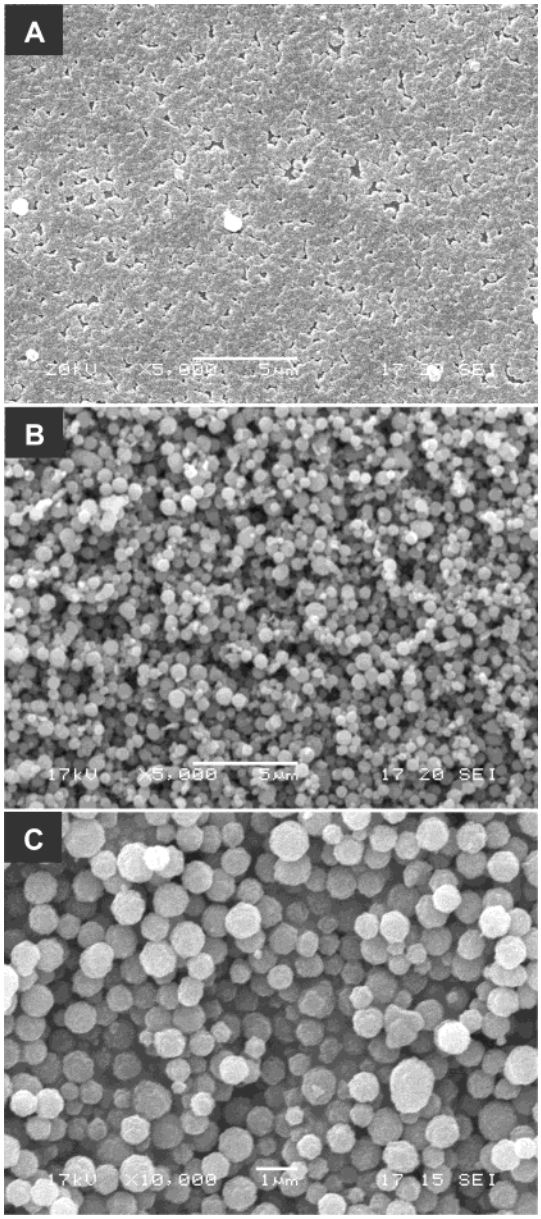

Figure 1. TiO_2 film (A) on the (010) surface of α-MoO_3 and unsupported TiO_2 spheres (B) prepared with 0.0040 M TiF_4 at 200 °C for 2 h. Unsupported TiO_2 spheres (C) obtained with 0.0020 M TiF_4 at 200 °C for 14 h.

When the TiF_4 is increased to 0.010 M, randomly arranged TiO_2 nanocrystallite films can also be formed on the (010) surface of α-MoO_3 substrate at a temperature as low as 55 °C after 3−6 h reactions, similar to the TiO_2 growth on silica substrate.[28]

When the TiF_4 solution is diluted to a regime of <0.0020 M, the growth of TiO_2 on the α-MoO_3 substrate becomes highly site-selective. As reported in Figure 2, nanocrystallites of TiO_2 of 80−200 nm were formed on the (010) surface of α-MoO_3. In particular, one-dimensional chainlike arrangements of TiO_2 crystallites can be observed at the "molecular steps" along the [001] direction of α-MoO_3,[26] as detailed in Figure 2B. One surprising observation on these TiO_2 nanostructures is that for certain areas of the same crystal surface, the growth of TiO_2 crystallites entirely ceased. For example, the surface of the crystal in Figure 2C (and similarly 2A) can be divided into two halves: the left side is totally free of TiO_2 while the right side is randomly scattered with tiny TiO_2 crystallites. On the basis on this observation, it is postulated that the area where no crystallites were grown must have higher crystal perfection, because crystal defects (e.g., point, line defects) normally act as preferred nucleation sites for the depositional growth. As further evidence to this conclusion, Figure 2D shows four different orientations of the lined TiO_2 crystallites (white lines) on the "molecular steps" of {001}, {100}, {101}, and {501} of α-MoO_3,[26] noting that the zigzag lines in the latter two high Miller indexed orientations are parallel. Occasionally, larger TiO_2 crystalline spheres (white spots in these SEM images) were grown on the (010) surfaces, even on the "perfect" crystal areas (e.g., circled area, upper left side, Figure 2A). The smaller crystallite size of TiO_2 in the defect area is due to a large amount of nucleation sites available with respect to a limited nutrient supply from the solution above. Therefore, only a few particles were developed into the large ones (Figure 2B,D).

Indeed, when highly crystalline α-MoO_3 substrate is used, the TiO_2 deposition becomes even more site-selective,[26] and the TiO_2 formation changes to a self-aligned growth mode. Figure 3 displays some of our experimental results in the present study. As can be seen, TiO_2 nanospheres in uniform sizes are formed exclusively. More importantly, while many uncovered areas can still be observed, the nanospheres are arranged compactly, forming hexagonal arrays on the (010) crystal plane of α-MoO_3. In some cases, surprisingly, this self-arrangement gives almost perfect hexagonal TiO_2 superlattices (e.g., Figure 3B) even without the surfactant assistance and the guidance of prepatterned substrate! It should be mentioned that the substrate crystal of Figure 3A−C was grown in the same batch of reaction as that of Figure 2. The self-organization of hexagonal TiO_2 arrays in Figure 3 indicates their growth mechanism is different from that of Figure 2, probably due to a higher degree of surface perfection. For those still have some intra-array spaces, the nanospheres are arranged largely in the hexagonal form. However, for those with denser packing, squarely arranged nanospheres can also be identified (Figure 3). These nanospheres might be formed in a less ideal growth environment due to limited surface space available, i.e., space constrain. One important observation here (Figure 3) is that there is no second layer buildup on the first layer nanospheres, unlike in the fast growth cases (Figures 1A and 2). The size (diameter) of the TiO_2 nanospheres is in the range of 100−1000 nm while most matured ones are in the regime of 500−600 nm. In certain experiments, hexagonal arrays of TiO_2 could be grown on the (010) surface of α-MoO_3 with a shorter reaction time but at a higher reaction temperature, as reported in Figure 3D. In such a case, the average diameter of spheres can be reduced to around only 250−300 nm. There is not much space between the spheres; some of the spheres were "forced" to grow into a hexagon-like shape (upper part of Figure 3D) in order to fully utilize the space, and certain interconnectivity among the spheres is clearly observable.

(28) Yang, H. G.; Zeng, H. C. *J. Phys. Chem. B;* Submitted for publication.

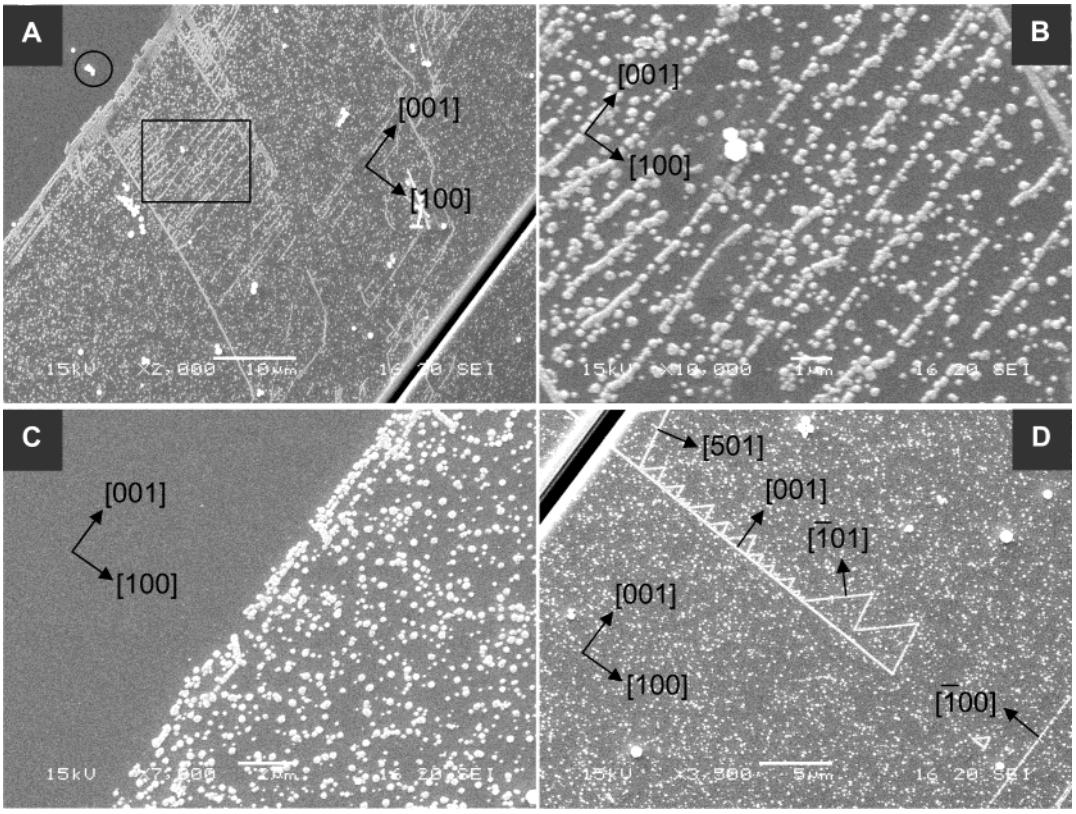

Figure 2. Site-selective growths of TiO_2 nanocrystallites on the (010) surface of α-MoO_3 single crystal: (A) growth on {100} "molecular steps"; (B) inset of (A); (C) growth on step-free surface; and (D) complex line pattern due to the growths on various "molecular steps". Experimental conditions: α-MoO_3 single crystals in 0.0013 M TiF_4 solution at 150 °C for 36 h.

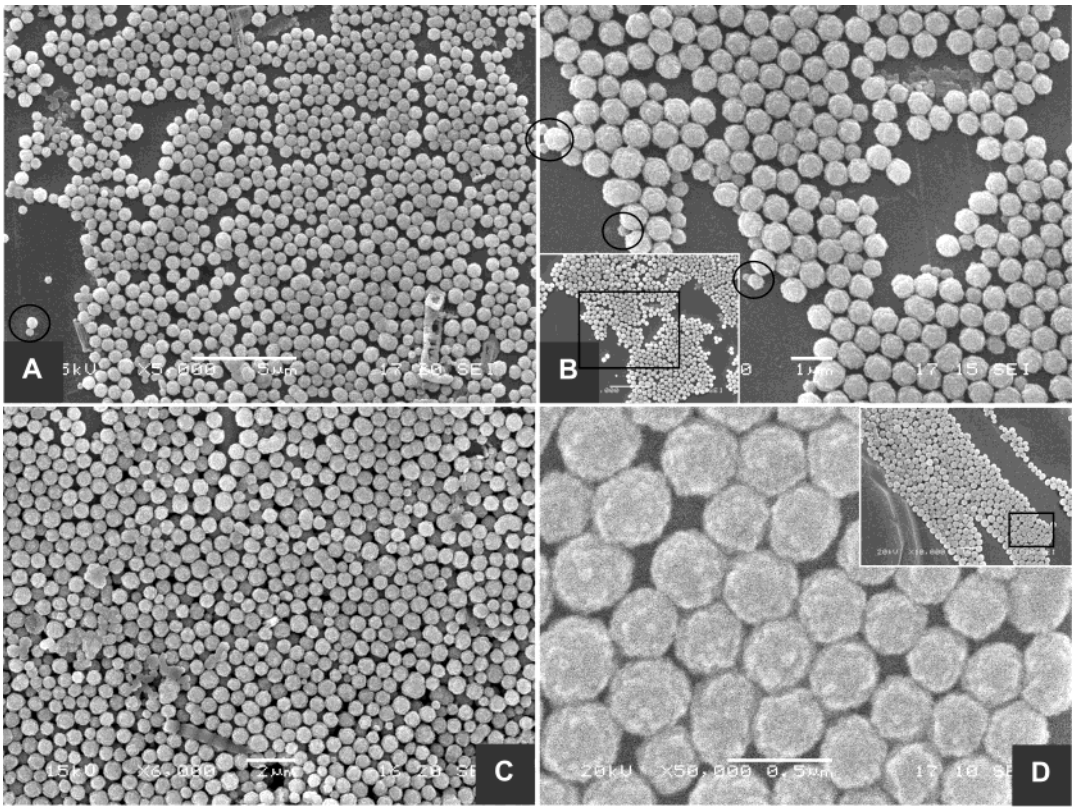

Figure 3. Self-aligned growths of hexagonal TiO_2 nanosphere arrays on the (010) surface of α-MoO_3 single crystals. Experimental conditions: (A−C) α-MoO_3 single crystals in 0.0013 M TiF_4 solution at 150 °C for 36 h. (D) α-MoO_3 single crystals in 0.0010 M TiF_4 solution at 200 °C for 14 h. Circled areas are discussed in Figure 5.

A number of factors can be attributed to the above self-aligned growths. First, the low concentration of TiF_4 precursor allows a selected nucleation only on the most energetically favorable α-MoO_3 sites. Second, the high

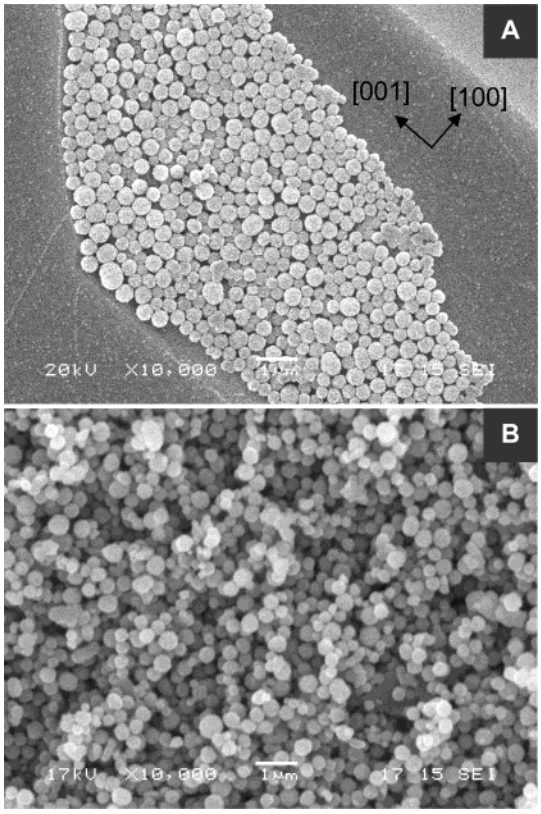

Figure 4. Self-alignment of hexagonal TiO_2 nanosphere arrays on the (010) surface of α-MoO_3 single crystals (A), and TiO_2 nanospheres grown from spontaneous nucleation (B); note that the nanospheres in (A) and (B) were prepared in the same batch of experiment with a 0.0010 M TiF_4 solution at 200 °C for 14 h.

degree of crystal perfection avoids multiple-nucleation across an entire surface (i.e., to prevent the random distribution of the TiO_2 in Figure 2). Third, the template effects of α-MoO_3 in directing and supporting the nanospheres are indispensable. As compared in Figure 4, the sizes of supported and unsupported TiO_2 nanospheres are essentially the same under the identical experimental conditions. This observation suggests that the overall growth rate depends largely on hydrothermal reactions rather than on solid templates, noting that there are many chemical equilibriums established among the two resultant TiO_2 phases (i.e., supported and unsupported) and solution chemical species. Nonetheless, it seems that the monodispersivity of the supported hexagonal TiO_2 nanosphere array might be slightly higher owing to the directing role of the α-MoO_3 support.

The highly organized arrays in a large-scale (Figures 3 and 4A) reveal that there exist certain growth mechanisms different from those found in normal organic surfactant-assisted oxide assemblies. First of all, unlike the post-growth particulate oxide assemblies that have been widely investigated these days, our hexagonal nanosphere arrays were generated in-situ during the hydrothermal reactions. Furthermore, inter-sphere connectivity (see Figures 3 and 4A, and TEM results in Figure 7), as a result of the continuous growth, indicates that the formation process of the arrays is not a discrete "growth-then-assembly" process, but an integrated "growth-cum-assembly" one. To explain this self-alignment process, we propose a continuous assembly mechanism, as shown in Figure 5, on the basis of experimental evidence from this work. In a first step, a cluster or crystal nucleus from the solution phase is crystallizing/landing on a defect site on the (010) surface of α-MoO_3 (a, Figure 5). The nucleus is growing into a larger sphere (b), while it creates a larger damaged area due to the chemical etching of hydrolysis products. Note that HF (which is a corrosive chemical etchant) is generated as a hydrolysis product from TiF_4 in producing TiO_2 (i.e., $TiF_4 + 2H_2O \rightarrow TiO_2 + 4HF$), which will create a localized HF-rich zone in the adjacent region of TiO_2 spheres. When the sphere reaches a critical dimension, the area created will then attract a new nucleus landing or a cluster crystallizing on it (c); the nucleus will later be developed into a larger one, and the new damaged area will become more inviting to a new nucleus (d). The repetition of the above steps will lead to formation of hexagonal arrays of the spheres (e and f, Figure 5).

The model proposed above is supported by a number of experimental observations. In Figures 3 and 4A, some nanospheres were fused into a low-dimensional lump or a dumbbell (two linked spheres) in certain defective areas as a result of rapid advance in the growth (steps c and d, Figure 5). Interestingly, paired TiO_2 spheres (one large and one small, as proposed in step c, Figure 5) have been actually observed in our SEM investigation (e.g., circled areas, Figure 3). Most importantly, these nanospheres, no matter whether they were isolated or fused, were grown according to their vicinity space available. On the other hand, the "critical sphere-size" (step c, Figure 5) has been evidenced in the hexagonal arrays where most of spheres indeed have similar spherical size (e.g., Figure 3B). Under our reaction conditions, these supported TiO_2 nanospheres were only formed as a monolayer, and the importance of the substrate to the continuous growth is unambiguously demonstrated. Interestingly, the "growth marks" (the defective areas underneath the nanospheres due to the HF etching and crystal growth; refer to Figure 5) have been indeed observed in some peeled area, i.e., removal of the nanospheres during the sample handling (see Supporting Information 1). Finally, HF chemical etching has been confirmed with blank α-MoO_3 single-crystals in a 10% HF aqueous solution for 5 min at room temperature. Our atomic force microscopic investigation reveals that the chemical etching with corrosive HF indeed causes a more defective (010) surface of acidic oxide α-MoO_3, using an unetched surface as reference (Supporting Information 2). The preferential growth of TiO_2 using the present precursor has been observed along an as-grown crystal edge (see Supporting Information 1) or an etched template surface.[28]

To further confirm the mechanism proposed in Figure 5, microcrystals of α-MoO_3 were also used as template for the self-aligned growth. With this microscale crystal substrate, total surface areas of α-MoO_3 can be significantly increased (a total of 0.30 g of the substrate was used in each run, with an estimated total surface area 7.8×10^{-2} m^2), compared to that of our single-crystal support (estimated total surface area 2.3×10^{-4} m^2) in Figures 2, 3, and 4. For TiF_4 solution at concentration of ≤0.0040 M (10−23 h, 170 °C), only nanocrystallites of TiO_2 can be formed on the surfaces of α-MoO_3, but these crystallites were not developed into nanospheres because of limited nutrient (TiF_4) supply in the solution.

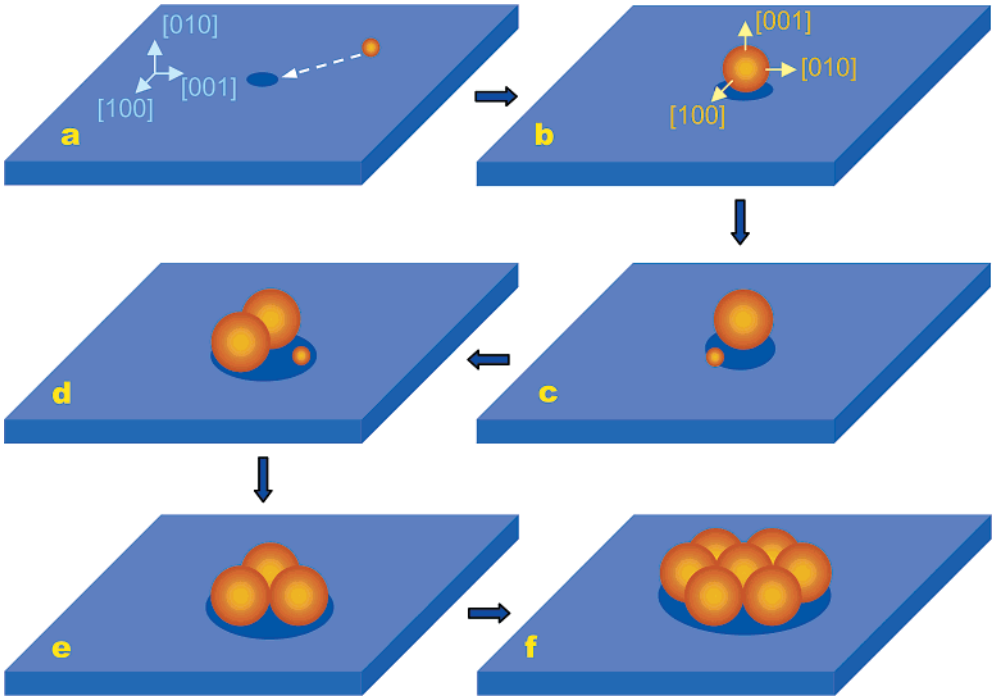

Figure 5. Self-aligned formation of hexagonal TiO_2 nanosphere arrays on α-MoO_3 substrate (in blue). Small and large orange spheres indicate small TiO_2 nuclei and matured nanospheres, respectively. The shadows (in deeper blue) underneath the TiO_2 spheres indicate defective areas due to the etching (not according to the actual sizes). The crystallographic orientations are determined in Figure 7.

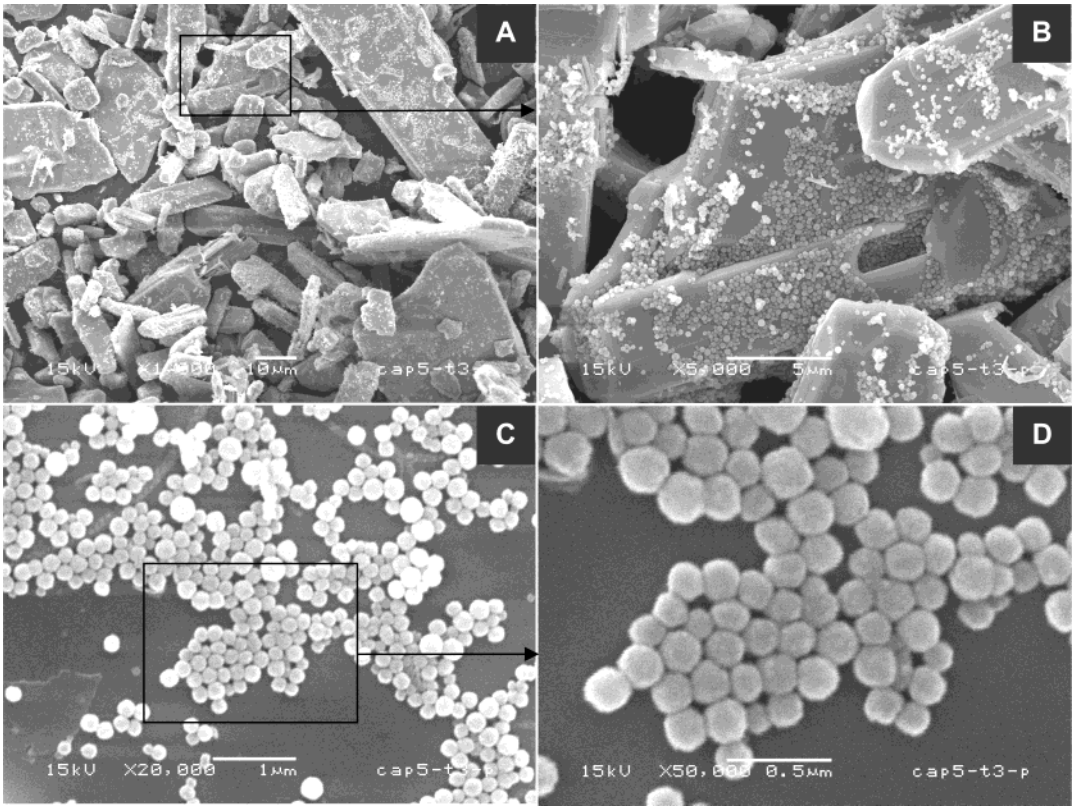

Figure 6. Self-alignment of hexagonal TiO_2 nanosphere arrays on the (010) surface of α-MoO_3 microcrystals at various magnifications: (A) overall morphology; (B) the inset of (A); (C) a detailed view on one of the microcrystal surfaces; and (D) the inset of (C). Experimental conditions: 0.30 g of α-MoO_3 microcrystals in 0.0050 M TiF_4 solution at 170 °C for 20 h.

However, similar hexagonal TiO_2 nanosphere arrays can be generated at TiF_4 solution concentrations of ≥0.0050 M. Figure 6 shows some of these growth results. Because of a much greater total substrate area available (more than 300 times!), TiO_2 crystallites were only grown into a spherical morphology on the α-MoO_3 microsupport (Figure 6A), and no unsupported TiO_2 spheres were found (clean deep dark background, Figure 6B). Because there are more nucleation centers (due to the large surface area), the resultant TiO_2 nanospheres do

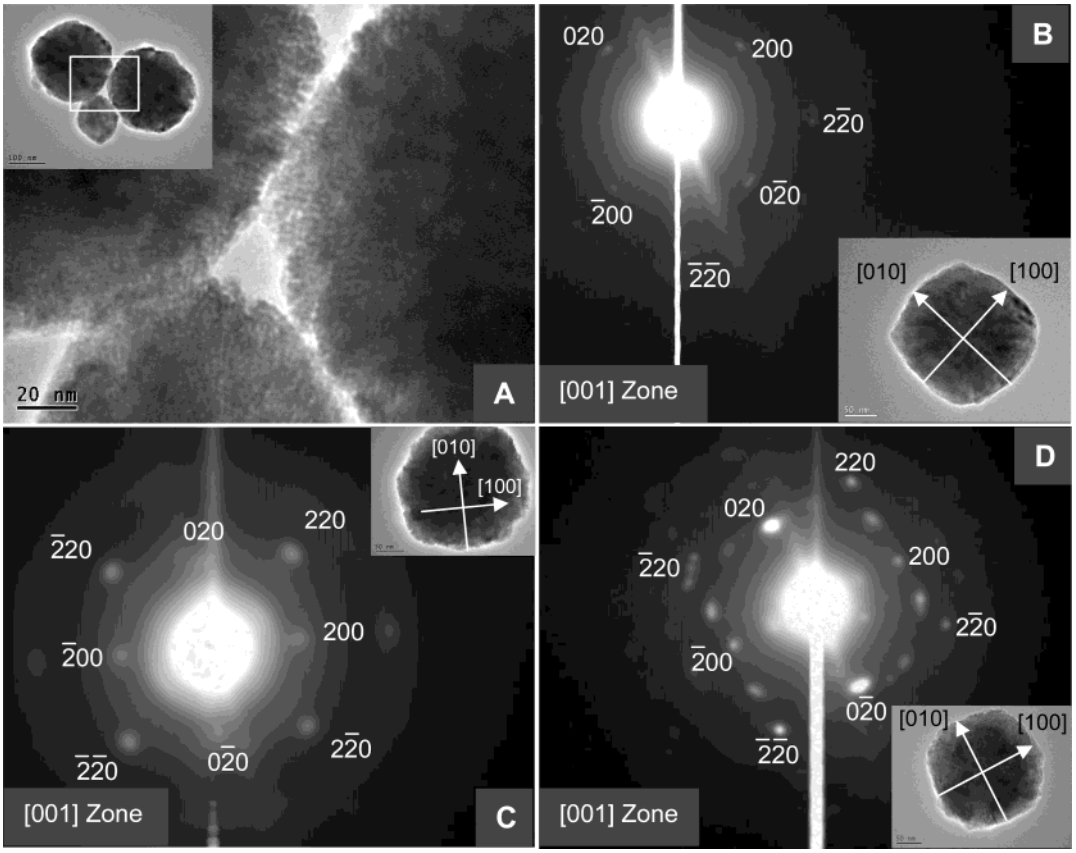

Figure 7. ED investigation on [001]-oriented TiO_2 nanospheres formed on the (010) surface of α-MoO_3 microcrystals. Experimental conditions: 0.30 g of α-MoO_3 microcrystals in 0.0050 M TiF_4 solution at 170 °C for 20 h (see Experimental Section for TEM sample preparation). Scale bars in the small TEM image insets are 100 nm (in A) and 50 nm (in B, C, and D).

not give large ordered arrays as those shown in the cases using large α-MoO_3 single-crystals. Compared to that of Figure 3, the regularity of array is poorer with the template of microcrystals (Figure 6D) because of a lowering in crystal quality. In a further confirmative experiment, the spontaneous nucleation of TiO_2 in solution phase was indeed taking place when the solution concentration was increased to 0.0133 M, producing both α-MoO_3-supported and unsupported TiO_2 nanospheres (Supporting Information 3). With all these comparative results, the "growth-then-assembly" process can be ruled out unambiguously, and the model proposed in Figure 5 is therefore validated.

The crystallographic phase has been further investigated with XRD and ED methods which reveal that the nanospheres prepared with this hydrothermal route are in anatase polymorph. In particular, all the major XRD diffraction peaks of anatase phase, (101), (004), (200), (105), and (204), can be observed (Supporting Information 4).[29] The hydrolysis formation of the anatase TiO_2 using TiF_4 precursor at acidic condition has been well-known in the literature,[28,30] regardless of the types of substrates (including polymeric materials). The chemical composition of the anatase TiO_2 from this type of synthesis is confirmed with EDX, which shows there is no impurity included (Supporting Information 5). Furthermore, our XPS analysis on binding energies of photoelectrons gives Ti $2p_{3/2}$ BE = 459.0 eV, Ti $2p_{1/2}$ BE = 464.6 eV, Mo $3d_{5/2}$ BE = 233.0 eV, Mo $3d_{3/2}$ BE = 236.2 eV, and O 1s BE = 530.7 eV.[30] As these BEs are identical to the literature data for the phase pure TiO_2 and MoO_3, it is known that there is no inter-diffusion or reactions between the cations in TiO_2 phase and α-MoO_3 substrate, owing to their large difference in oxidation states (Supporting Information 6).[30,31]

The crystal orientation of the TiO_2 nanospheres is further determined with a TEM/ED technique. Figure 7A shows a detailed juncture area among three spheres. Some spheres are clearly in contact with each other using their outer curvatures while others seem to be quite isolated (inset). Among the individual spheres examined, most spheres show single-crystalline characteristics, as reported in Figure 7B and C. The ED patterns can be indexed into diffraction spots of the [001] zone, which implies that the crystal spheres are standing on the substrate surface with their [001] axis parallel to the [010] of α-MoO_3 (Figure 5). It should be pointed it out that, statistically, most TiO_2 nanospheres give this type of square diffraction patterns; note that these TiO_2 nanospheres would use their flat base (i.e., the (001) plane which was formed in contact with the α-MoO_3 support) for settlement during TEM sample preparation (see Experimental Section). In some cases, as shown for example in Figure 7D, additional diffraction spots (not indexed, such as 101 spots near the

(29) Joint Committee on Powder Diffraction Standards, International Centre for Diffraction Data, Card No. 21-1272, Swarthmore, PA, 1996.

(30) Lou, X. W.; Zeng, H. C. *J. Am. Chem. Soc.* **2003**, *125*, 2679.

(31) Elder, S. H.; Cot, F. M.; Su, Y.; Heald, S. M.; Tyryshkin, A. M.; Bowman, M. K.; Gao, Y.; Joly, A. G.; Balmer, M. L.; Kolwaite, A. C.; Magrini, K. A.; Blake, D. M. *J. Am. Chem. Soc.* **2000**, *122*, 5138.

central beam) are also shown up in the same [001] zone spots, which indicates that this sphere is composed of more than one crystallite, i.e., it is polycrystalline. Nonetheless, a predominant orientation for this sphere is still along the [001] axis, judging from the overall ED intensity. The observed crystallographic orientations had also been confirmed very recently by us using the α-MoO_3 nanorod template,[30] which also shows that the [100] and [010] of anatase TiO_2 are parallel to the [100] and [001] of α-MoO_3, respectively (indicated in Figure 5). The preferred orientation of [001] is understandable, because the lattice mismatch between the (001) plane of anatase TiO_2 and the (010) surface of α-MoO_3 is small (anatase TiO_2, tetragonal symmetry, $a = 3.7852$ Å and $c = 9.5139$ Å; α-MoO_3, orthorhombic, $a = 3.9630$ Å, $b = 13.856$ Å, and $c = 3.6966$ Å).[30,31] The [001] crystal orientation is also in favor of formation of spherical type morphology, because anatase TiO_2 belongs to the tetragonal symmetry (i.e., lattice constants $a = b$), and a high symmetry can still be maintained in the [001] standing TiO_2 spheres. As a further confirmation, flattening (i.e., the formation of (001) surface) of [001]-oriented TiO_2 spheres has been indeed observed in some larger spheres (see Supporting Information 1).

Although the individual TiO_2 nanospheres stand preferably along the [001] axis, the overall hexagonal arrays of the nanospheres do not show preferential crystallographic orientations with respect to the underneath α-MoO_3, i.e., the unit vectors of the hexagonal superlattices do not show definite relationships with those of the substrate. This observation seems to suggest that similar organizations could also be achieved on other metal oxide substrates as long as the synthetic parameters are carefully examined. As revealed in this study, high crystallinity of substrate and slow hydrolysis rate are the two key controlling factors. In particular, self-generated etchant HF along the way of nanosphere formation provides the nucleation centers for the subsequent nanosphere growth. In this sense, the localized HF works like a chemical "bulldozer" to pave new paths ahead for the self-expanding "growth-cum-assembly". Apart from the substrate search and selection, furthermore, other metal fluorides may seem to be suitable precursors for new metal oxide arrays. Although we have achieved almost perfect hexagonal arrangement in certain cases (e.g., Figure 3B), a further improvement on the array ordering is still needed. Apparently, there are tremendous challenges for future research of this synthetic scheme. Nonetheless, as a first step toward this end, the current investigation has shown us the possibility of direct organization of oxide superlattices on the simple single-crystal planes.

Conclusion

In summary, without the assistance of organic surfactants and substrate prefabrication, direct fabrication of hexagonal superlattice arrays of anatase TiO_2 nanospheres on the (010) crystal plane of α-MoO_3 can be achieved by hydrolysis of TiF_4 precursor under hydrothermal conditions at 150−200 °C. This novel ordered scheme allows a concurrent growth and self-alignment of TiO_2 nanospheres on the metal oxide substrates. On the basis of various growth experiments and materials characterization, two important synthetic parameters have been identified in this work: (i) high crystallinity of substrate, and (ii) low hydrolysis rate. On the other hand, the localized enrichment of hydrolysis product HF is concluded to play a crucial role in generating the heterogeneous nucleation and directing the self-alignment of the oxide arrays, as proposed in the "growth-cum-assembly" mechanism. On the basis of these findings, it has been indicated that this direct assembly scheme may be extendable to new material combinations using other metal fluorides and single-crystal oxide substrates.

Acknowledgment. We gratefully acknowledge the financial support of the Ministry of Education, and Agency for Science, Technology and Research, Singapore.

Supporting Information Available: SEM images, AFM images, XRD patterns, EDX microanalysis, and XPS spectra of representative crystals, nanospheres, and substrates that are the subject of this study (PDF). This material is available free of charge via the Internet at http://pubs.acs.org.

CM034313F